ACS Catalysis

pubs.acs.org/acscatalysis

Research Article

A Bifunctional Iron Nanocomposite Catalyst for Efficient Oxidation of Alkenes to Ketones and 1,2-Diketones

Tao Song, Zhiming Ma, Peng Ren, Youzhu Yuan, Jianliang Xiao,* and Yong Yang*

Cite This: *ACS Catal.* 2020, 10, 4617−4629

Read Online

ACCESS | Metrics & More | Article Recommendations | Supporting Information

ABSTRACT: We herein report the fabrication of a bifunctional iron nanocomposite catalyst, in which two catalytically active sites of Fe−N_x and Fe phosphate, as oxidation and Lewis acid sites, were simultaneously integrated into a hierarchical N,P-dual doped porous carbon. As a bifunctional catalyst, it exhibited high efficiency for direct oxidative cleavage of alkenes into ketones or their oxidation into 1,2-diketones with a broad substrate scope and high functional group tolerance using TBHP as the oxidant in water under mild reaction conditions. Furthermore, it could be easily recovered for successive recycling without appreciable loss of activity. Mechanistic studies disclose that the direct oxidation of alkenes proceeds via the formation of an epoxide as intermediate followed by either acid-catalyzed Meinwald rearrangement to give ketones with one carbon shorter or nucleophilic ring-opening to generate 1,2-diketones in a cascade manner. This study not only opens up a fancy pathway in the rational design of Fe−N−C catalysts but also offers a simple and efficient method for accessing industrially important ketones and 1,2-diketones from alkenes in a cost-effective and environmentally benign fashion.

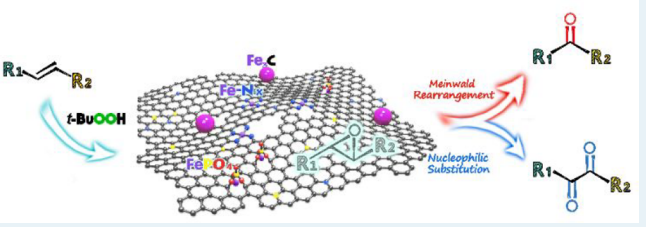

KEYWORDS: *bifunctional catalysis, iron nanocomposites, alkenes oxidation, ketones, 1,2-diketones*

1. INTRODUCTION

Ketones, including 1,2-diketones, are very important and useful intermediates or building block in synthetic organic chemistry, pharmaceuticals, agrochemicals, and bulk/fine chemicals.[1] While many methods have been developed for the preparation of ketones, those that employ alkenes as the substrate are particularly appealing, as they are one of the most fundamental and most easily accessible chemicals. Indeed, alkenes have been used as starting materials for the synthesis of ketones over the past decades. However, only a handful of examples have been reported to date of preparing ketones and 1,2-diketones from *trans*-disubstituted alkenes via catalytic oxidation (Scheme 1).[2,3] Furthermore, the methods developed generally suffer from such disadvantages as limited alkene scope, cost and toxicity of the metal catalysts and/or oxidants, difficult product/catalyst separation, and environmental compatibility. Therefore, it is highly desirable to develop new approaches for the oxidation of alkenes into ketones and 1,2-diketones in a cost-effective and environmentally benign manner.

It has been well-documented that epoxides can be transformed into ketones, 1,2-diols, 1,2-diketones, carboxylic acids, or other novel molecules via either facile C−O cleavage or challenging C−C bond cleavage under various conditions, such as the nucleophilic ring-opening to generate 2-hydroxyalkylated derivatives,[4] the acid-catalyzed Meinwald rearrangements to yield carbonyl compounds,[5] or the strong base-promoted isomerization to give allylic alcohols.[6] Considering that epoxides are readily available from alkenes via a one-step oxidation process,[7] we thought that direct oxidation of alkenes to afford ketones and/or 1,2-diketones might be realized in a cascade manner via the formation of epoxides as an intermediate followed by acid/base catalysis or nucleophilic ring-opening (Scheme 1).

The key to this strategy is the rational design and preparation of a bifunctional catalyst, in which active redox and acid/basic sites are integrated into a single catalyst to cooperatively enable the cascade epoxidation and ring-opening reactions in a sequential manner. Two such proof-of-concept catalysts have been reported and have demonstrated the potential for the reaction.[2a,b] However, they suffer from the issues of restricted substrate scope, demanding reaction conditions, and low catalyst stability, which significantly impede their practicability in chemical synthesis. Therefore, a more efficient bifunctional catalyst, ideally a heterogeneous one, which allows for the oxidation of alkenes into ketones with high activity and productivity, expanded scope, easy catalyst/product separation, and milder reaction conditions is urgently needed.

Received: December 2, 2019
Revised: March 23, 2020
Published: March 25, 2020

Scheme 1. Synthesis of Ketones and 1,2-Diketones from Oxidation of Alkenes

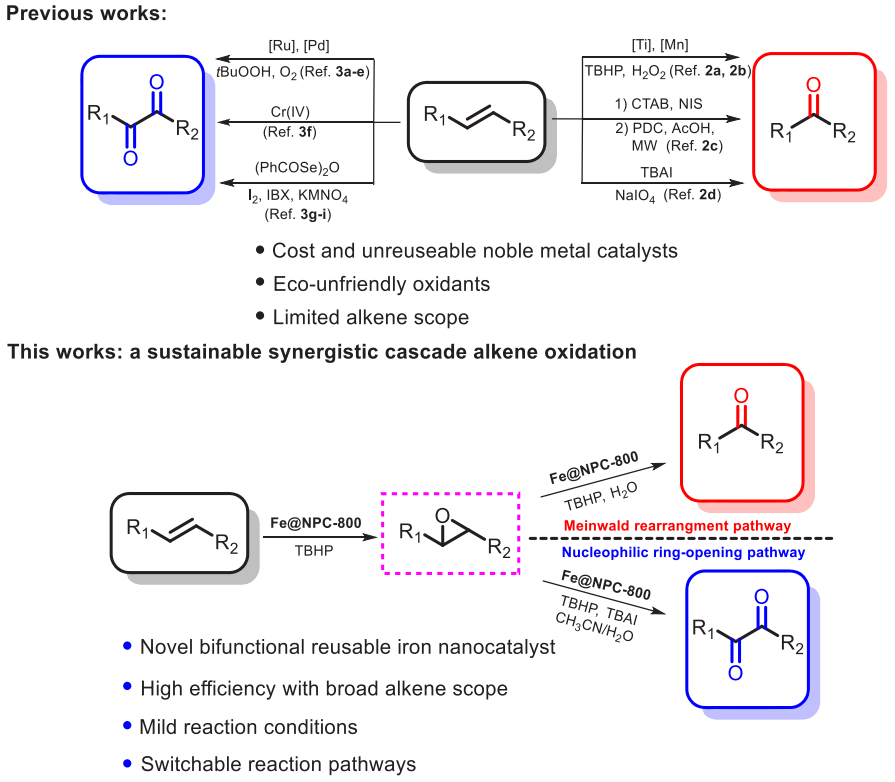

Herein, we report a facile and easily scalable method to prepare a bifunctional iron nanocomposite, in which two catalytically active iron species, i.e., Fe−N_x and $FePO_4$, as redox and Lewis acid sites coexist on the surface of hierarchical N,P-dual doped porous carbon. With inexpensive and biocompatible iron as the active site, the nanocomposite enables synergistically cooperative catalysis for the oxidation of various alkenes into ketones and 1,2-diketones in high yields with *tert*-butyl hydroperoxide (TBHP) as the oxidant in water or a CH_3CN−water mixture under mild reaction conditions. Furthermore, the catalyst can be readily recovered for re-use without appreciable loss of catalytic performance.

2. CATALYST PREPARATION AND CHARACTERIZATION

2.1. Catalyst Preparation. The iron nanocomposite catalysts were prepared in a facile and environmentally benign manner following our recently developed method that starts from naturally available and renewable biomass as nitrogen and carbon sources (see the Supporting Information for the details).[8] Typically, fresh bamboo shoots were first cut into slices, dried, and grounded into powder, followed by a hydrothermal process. The resulting solids were homogeneously mixed with $Fe(NO_3)_3$ and PPh_3, as Fe and P sources, respectively, followed by pyrolysis under a N_2 atmosphere at varying temperatures to obtain the iron nanocomposites catalysts, hereinafter denoted as Fe@NPC-*T* (where *T* represents the pyrolysis temperature, e.g., 700, 800, and 900 °C). The iron contents were determined to be 5.0 wt % for Fe@NPC-700, 5.8 wt % for Fe@NPC-800, and 7.0 wt % for Fe@NPC-900, respectively, by coupled plasma optical emission spectrometry (ICP-OES) (Table S2).

2.2. Catalyst Characterization. The transmission electron microscope (TEM) and high-resolution images (Figure 1A−I) for the catalysts Fe@NPC-*T* show that metallic iron nanoparticles (NPs) containing Fe and/or Fe_3C crystalline phases with uniform size were evenly dispersed on graphitic carbon. The high-angle annular dark-field scanning transmission electron microscopy (HAADF-STEM) images and energy-dispersive X-ray (EDX) maps (Figure 1J) reveal that Fe, N, P, O, and C atoms were homogeneously distributed as well. X-ray diffraction (XRD) patterns (Figure S1A) and magnetic measurements (Figure S2) verify that the metallic Fe and/or Fe_3C NPs were supported on graphitic carbon. Two characteristic D and G bands at 1590 and 1350 cm^{-1} in the Raman spectra (Figure S1B) provided solid evidence for the formation of graphitic carbon with a certain degree of graphitization and varying defected sites.[8] N_2 adsorption/desorption measurements demonstrate that the catalysts Fe@NPC-*T* possess hierarchically micro-, meso-, and macropores with high specific surface areas and large pore volumes (Figure S3 and Tables S1 and S2).

The nature of N, P, and Fe in Fe@NPC-*T* was studied by X-ray photoelectron spectroscopy (XPS; Figure 2a,b and Figure S4). The N 1s spectrum contains five peaks at 398.02, 399.6, 400.4, 401.3, and 402.5 eV, which are assigned to pyridinic, Fe−N_x, pyrrolic, quaternary, and oxidized N, respectively (Figure 2a). The content of each type of nitrogen varies as the pyrolysis temperature increases (Table S3). Of the peaks, the one at 399.6 eV is in good consistence with that of ironphthalocyanine (FePc), indicating that Fe coordinates with N atoms in aromatics to form catalytically active Fe−N_x sites.[9] This observation also clearly suggests that the N atoms are incorporated into the carbon lattice. Three types of P species could be identified from the P 2p spectrum, that is, Fe−P (zero valence state, 129.2 and 130.4 eV),[10] P−C (132.8 eV),[8d,11] and PO_3^- and PO_4^{3-} (5+, 133.7 and 134.4 eV)[11] (Figure S4). The formation of $FePO_4$ was further supported by

https://dx.doi.org/10.1021/acscatal.9b05197
ACS Catal. 2020, 10, 4617−4629

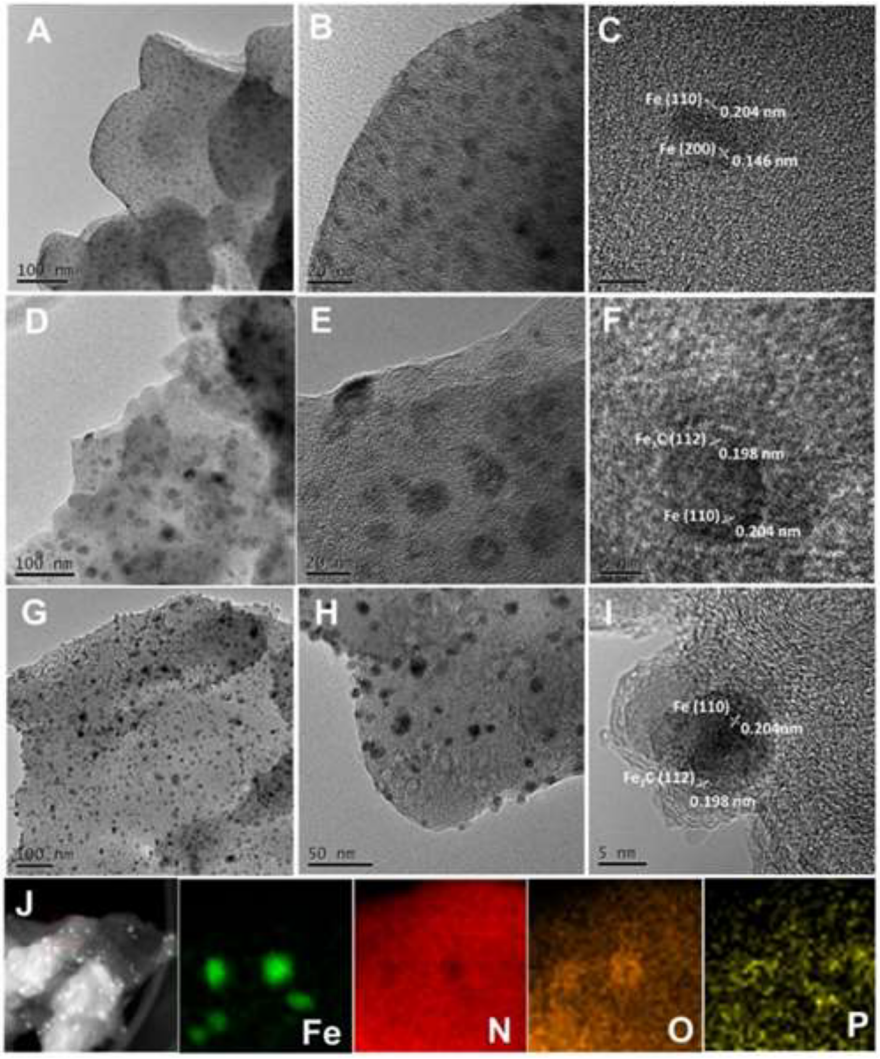

Figure 1. (A, B) TEM images of Fe@NPC-700 and (C) HR-TEM image of Fe@NPC-700. (D, E) TEM images of Fe@NPC-800 and (F) HR-TEM image of Fe@NPC-800. (G, H) TEM images of Fe@NPC-900 and (I) HR-TEM image of Fe@NPC-900. (J) HAADF STEM image and corresponding EDX mappings of Fe, N, O, and P of Fe@NPC-800.

a FT-IR experiment with an appearance of a characteristic band at 1045 cm^{-1}, assignable to the stretching of the P−O bond present in PO_4^{3-} (Figure S7).[12] The Fe 2p XPS spectra (Figure 2b) were fitted into three peaks at 706.8, 710.4, and 712.0 eV, respectively. The peak at 706.8 eV can be attributed to zero valence Fe (metallic iron or carbide).[9b,13] The peak at 710.4 eV can be assigned to Fe in Fe−N_x configuration, while the peak at 712.0 eV can be indexed to Fe^{3+} in $FePO_4$.[14] A notable positive shift in the binding energy assignable to Fe−N_x configuration in Fe@NPC-*T* compared with that of FePc implies interactions of Fe−N_x with metallic iron NPs.[9b] Noticeably, the content for each iron species in the Fe@NPC-*T* varies with pyrolysis temperatures.

X-ray absorption measurements were further performed to analyze the coordination environment of Fe at the atomic level. The near-edge absorption energy position of Fe@NPC-*T* was located between that of Fe foil and $FePO_4$ in Fe K-edge absorption near-edge structure (XANES) suggests that the valence state of Fe is in between 0 and +3 (Figure 2c). This is in agreement with the XPS results. The Fourier transform (FT) k^3-weighted EXAFS spectra of Fe@NPC-*T* show one main peak at around 1.5 Å, which belongs to the first coordination shell of Fe−N and is notably similar to that of FePc, suggesting that they are more likely to form Fe−N_x coordination structures (Figure 2d).[9b,15] Besides, the peak at around 2.5 Å, ascribed to the Fe−C distance of the second neighbor shell, was also observed.[9b] However, the spectrum of Fe@NPC-700 is more similar to Fe foil, with two strong peaks at around 2.1 and 4.5 Å, which correspond to the Fe−Fe distance,[9b] revealing the presence of metallic iron crystalline structures. The peak of the Fe−Fe bond could also be observed in Fe@NPC-800 and Fe@NPC-900, corroborating that metallic iron exists in both samples, which is consistent with the HR-TEM and XRD results. Noticeably, the EXAFS spectrum of either Fe@NPC-800 or Fe@NPC-900 shows a higher peak intensity for Fe−N bonding and a lower intensity for Fe−Fe bonding compared to those of Fe@NPC-700. Nonetheless, these data suggest that Fe−N_x configurations are incorporated in the graphitic carbon frameworks in the catalysts and their intensity increases with the increase of pyrolysis temperatures.

https://dx.doi.org/10.1021/acscatal.9b05197
ACS Catal. 2020, 10, 4617−4629

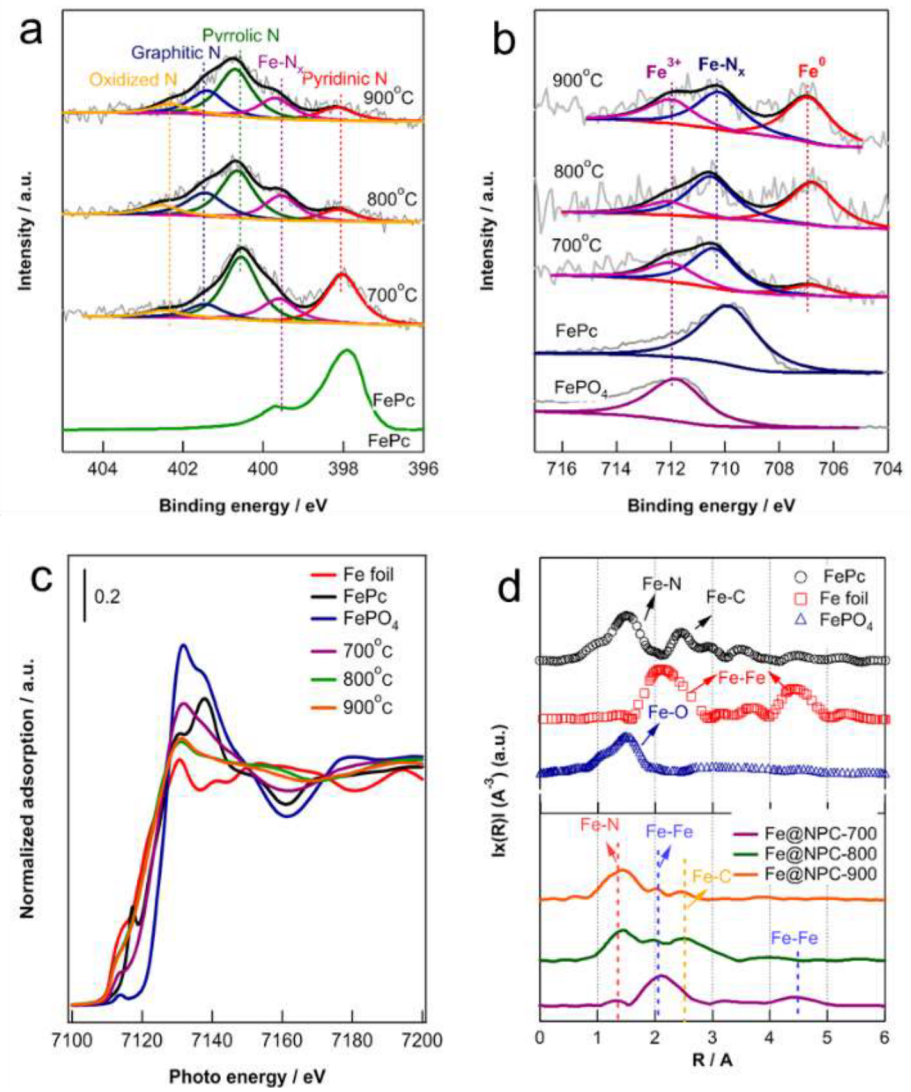

Figure 2. High-resolution XPS spectra of (a) N 1s and (b) Fe 2p for Fe@NPC-700, -800, and -900. (c) Fe K-edge XANES and (d) Fourier transform (FT) EXAFS spectra of Fe@NPC-700, -800, and -900, with FePc, Fe foil, and $FePO_4$ as references.

3. RESULTS AND DISCUSSION

3.1. Oxidation of Alkenes to Ketones. To examine the catalytic activity of the iron nanocomposite Fe@NPC-*T* for the oxidative cleavage of alkenes, *trans*-stilbene **1a** was chosen as a model substrate (Table 1). The reaction was performed in the presence of Fe-@NPC-800 as a catalyst and 5 equiv of TBHP as an oxidant at 100 °C in water. To our delight, full conversion of **1a** with the formation of one-carbon shorter benzophenone **2a** as major product in 86% selectivity was observed (entry 1 in Table 1). The selectivity to **2a** as high as 92% could be achieved with 98% conversion of **1a** at 90 °C under otherwise identical conditions (entry 2 in Table 1). However, a further decrease of the reaction temperature to 80 °C led to a rather lower reactivity (entry 3 in Table 1). Lowering the amount of TBHP (e.g., 3 equiv with respect to **1a**) drastically decreased the reactivity too (entry 4 in Table 1). By using hydrogen peroxide, air, or molecular oxygen instead of TBHP as the terminal oxidant, no reaction was observed with full recovery of **1a** under identical conditions (entries 5−7 in Table 1). Further screening of the as-prepared catalysts, e.g., Fe@NPC-700 and Fe@NPC-900, revealed that the pyrolysis temperature for the preparation of the iron nanocomposite has an important influence on the reactivity (entries 8 and 9 in Table 1), with Fe@NPC-800 affording the best result. Control experiments employing commercially available Fe_2O_3, Fe_3O_4, $Fe(NO_3)_3$, $FePO_4$, iron phthalocyanine (FePc), and nano Fe powder as catalysts for the reaction all showed inferior reactivity with the formation of a mixture of products (entries 11−16 in Table 1). In addition, when NPC-800 without the introduction of iron was employed as a catalyst, no reaction was observed under the same conditions, indicating the essential role of the Fe@NPC-*T* in catalysis (entry 17 in Table 1). Therefore, the optimized conditions are as follows: Fe@NPC-800 as a catalyst, TBHP (5 equiv with respect to *trans*-stilbene) as an oxidant, 90 °C in water. Of note, the carbon balance closure is nearly 90% for the benchmark reaction under different conditions, as shown in Table S9.

After identifying the optimal reaction conditions, we next investigated the generality of this protocol, as shown in Table 2. Overall, a variety of alkenes could efficiently undergo the selective cleavage reaction to afford their corresponding one-carbon shorter ketones in high yields with good tolerance of

https://dx.doi.org/10.1021/acscatal.9b05197
ACS Catal. 2020, 10, 4617−4629

Table 1. Optimization of Reaction Conditions for Synthesis of Ketones[a]

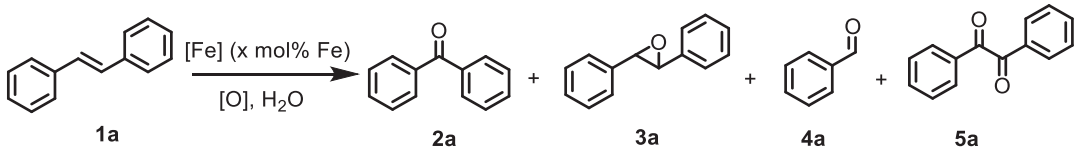

entry	catalyst	oxidant	T [°C]	conversion [%][b]	selectivity [%][b] 2a	3a	4a	5a
1	Fe@NPC-800	TBHP	100	100	86	0	10	0
2	**Fe@NPC-800**	**TBHP**	**90**	**98**	**92**	**0**	**4**	**2**
3	Fe@NPC-800	TBHP	80	57	65	12	14	9
4[c]	Fe@NPC-800	TBHP	90	43	91	0	9	0
5	Fe@NPC-800	H_2O_2	90	0				
6	Fe@NPC-800	air	90	0				
7[d]	Fe@NPC-800	O_2	90	0				
8	Fe@NPC-700	TBHP	90	79	42	47	11	0
9	Fe@NPC-900	TBHP	90	100	71	10	11	0
10	Fe@NC-800	TBHP	90	90	59	24	17	0
11	Fe_2O_3	TBHP	90	19	32	68	0	0
12	Fe_3O_4	TBHP	90	23	30	48	22	0
13	Fe powder	TBHP	90	11	45	28	27	0
14	$Fe(NO_3)_3$	TBHP	90	7	71	29	0	0
15	FePc	TBHP	90	31	41	37	22	0
16	$FePO_4$	TBHP	90	11	77	7	16	0
17	NPC-800	TBHP	90	0				

[a]Reaction conditions: *trans*-stilbene (0.2 mmol), catalyst (10 mol % of Fe), oxidant (5 equiv), H_2O (4 mL), 90 °C, 12 h. [b]Determined by GC−MS. [c]TBHP (3 equiv). [d]Oxygen balloon.

various functional groups. Electron-donating group-substituted 1,2-diarylalkenes gave higher yields than those substituted by electron-withdrawing groups, e.g., $-NO_2$ (**1i**), −CN (**1j, 1k**), and $-CF_3$ (**1l**). Halogen-substituted 1,2-diarylalkenes (**1b−e**) tolerate the present conditions, and the respective diaryl ketones were achieved in 80%−87% yields with no undesired dehalogenation taking place. Other functional groups, e.g., PhthN− (**1m**), $-NH_2$ (**1n**), −COOH (**1o**), and MeO_2C- (**1p**), were also compatible with the present conditions. Delightfully, 2,3,4,5,6-pentafluoro-substituted 1,2-diarylalkene (**1r**) also worked well to produce 2,3,4,5,6-pentafluorobenzophenone with a decent yield, which is frequently used in the synthesis of OLED[16] and F-containing polymers.[17] More importantly, heterocycle-substituted internal alkenes, such as 2-styrylthiophene (**1t**) and 2-styrylpyridine (**1s**), are compatible with this catalytic system, delivering their respective ketones in 71% and 77% yield, respectively. These results indicate that this method is highly useful for the preparation of pharmaceuticals and functional materials. Furthermore, aryl- and alkyl-substituted unsymmetric alkenes (**1u−z**) could undergo the oxidative cleavage reaction to selectively produce their corresponding ketones in good yields under the optimized conditions. In addition, various substituted styrenes (**1ab−ae**) work well to produce its corresponding aldehyde as the final product. For those 1,1-disubstituted terminal alkenes, e.g., ethene-1,1,2-triyltribenzene (**1af**), (*E*)-prop-1-ene-1,2-diyldibenzene (**1ag**), and 1,1,2-trisubstituted alkenes, e.g., ethene-1,1-diyldibenzene (**1ah**), prop-1-en-2-ylbenzene (**1ai**), they were converted into their corresponding one-carbon shorter ketones and tertiary alcohols (**2af−ag**) in satisfactory yields, respectively. However, for dialkyl substituted alkene, e.g., 2-octene (**1aa**), a mixture of its corresponding epoxide, aldehyde, and acid was observed with no formation of the desired ketone, mainly due to the higher oxidation potential of aliphatic acids than benzyl carboxylic acids, which is unfavorable for the oxidative decarboxylation of aliphatic acids to the corresponding carbon radical and subsequent cascade oxidation process.[18]

3.2. Oxidation of Alkenes to 1,2-Diketones. In the course of the condition optimization for the reaction of *trans*-stilbene **1a** catalyzed by Fe@NPC-800, benzil (**5a**) was detected, albeit with considerably lower yield (Table 1, entries 2 and 3). This finding indicates that 1,2-diketones could be synthesized from alkenes if appropriate conditions are in place. Therefore, we attempted to synthesize 1,2-diketones from alkenes under the catalysis of Fe@NPC-800 by modification of the reaction conditions.

With **1a** still as the model substrate, a set of parameters including solvent, additive, temperature, and oxidant were intensively screened, and the results are compiled in Table S6 and Figure S11. To our pleasure, in the presence of 30 mol % of TBAI, 83% of isolated yield to benzil **5a** was achieved using Fe@NPC-800 (10 mol % of Fe) as a catalyst, 5 equiv of TBHP as an oxidant (with respect to **1a**), CH_3CN/H_2O (15/1, v/v) as solvent at 90 °C. Note that TBAI was employed as an additive because of the well-known capacity of iodide as a good nucleophilic and leaving group.[3e,f,19] With the optimized conditions in hand, we subsequently explored the generality of this method to selectively convert various alkenes to into 1,2-diketones. As shown in Table 3, all the stilbenes examined could be efficiently converted to their corresponding 1,2-diketones in high yields. A variety of functional groups, such as halides (**1b−d**), Me− (**1e**), MeO− (**1g** and **1h**), −CN (**1j** and **1k**), CF_3- (**1l**), and NO_2- (**1i**), and MeO_2C- (**1p**), are all tolerated. 2,3,4,5,6-Pentafluoro-substituted 1,2-diarylalkene (**1r**) also worked well to produce **5m** in satisfactory yield.

https://dx.doi.org/10.1021/acscatal.9b05197
ACS Catal. 2020, 10, 4617−4629

Table 2. Substrate Scope of Alkenes for Synthesis of Ketones[a]

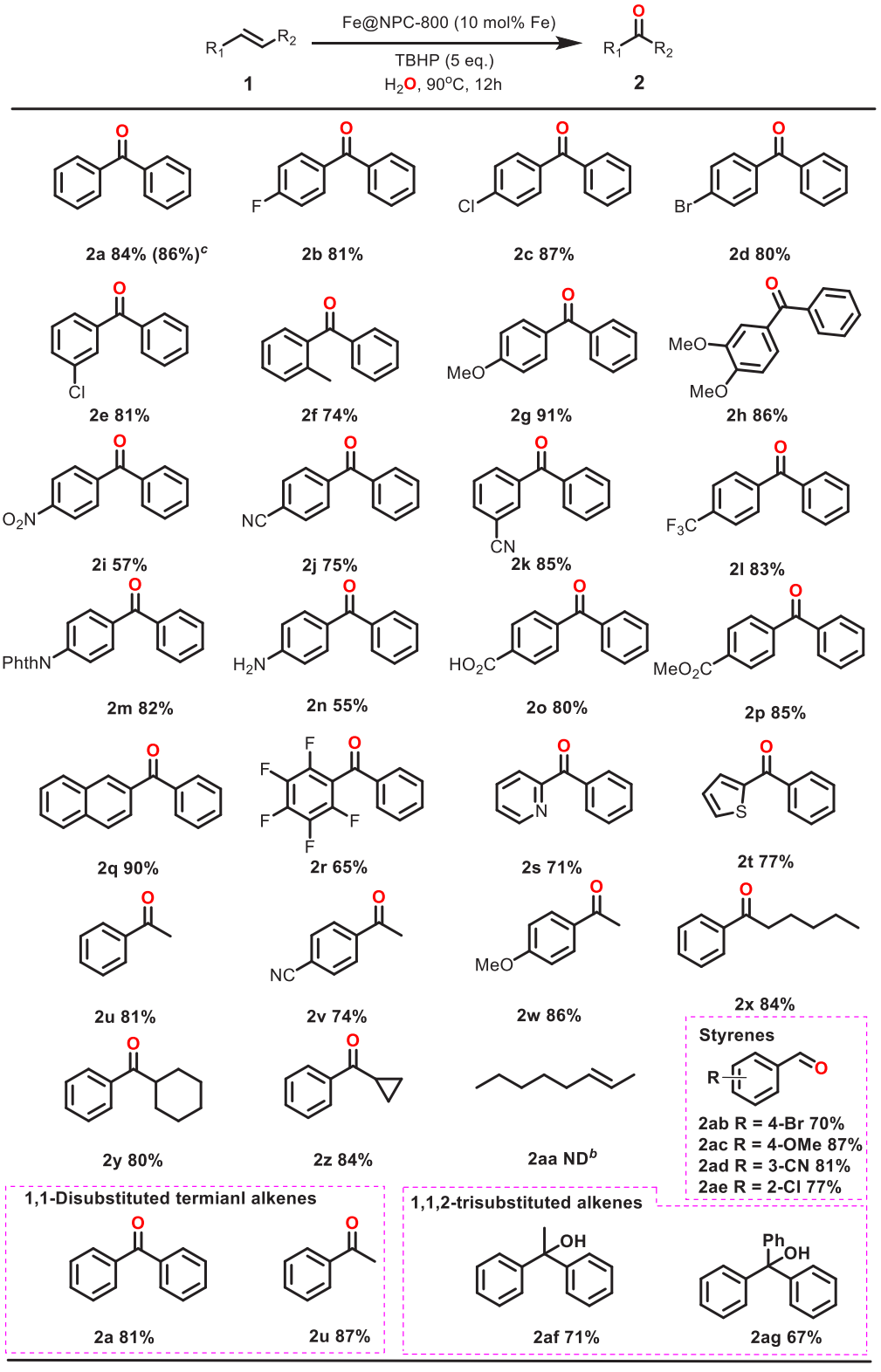

[a]Reaction conditions: alkene (0.2 mmol), catalyst (10 mol % of Fe), TBHP 70 wt % in water (5 equiv), H_2O (4 mL), 90 °C, 12 h. [b]No detected. [c]*cis*-Stilbene was used instead. Yields of isolated product are reported.

(*E*)-2-Styrylnaphthalene (**1q**) and heteroatom-containing alkene, 2-styrylthiophene (**1t**), were efficiently converted to their corresponding 1,2-diketones in high yields. Notably, 1-((*E*)-2-(cyclohexa-1,5-dien-1-yl)vinyl)-4-((*E*)-styryl)benzene (**1o**) containing two C═C bonds was smoothly oxidized into **5o** in 74% yield with 10 equiv of TBHP and 24 h. Aryl- and alkyl-substituted unsymmetric alkenes (**1q'**, **1r'**, **1u**, and **1x−z**) also worked well to deliver their respective 1,2-diketones in 57%−81% yields. More surprisingly, styrene (**1w'**) was directly oxidized into phenylglyoxylic acid (PGA) **5w** in 57% yield, a

https://dx.doi.org/10.1021/acscatal.9b05197
ACS Catal. 2020, 10, 4617−4629

Table 3. Substrate Scopes of Alkenes for Synthesis of 1,2-Diketones

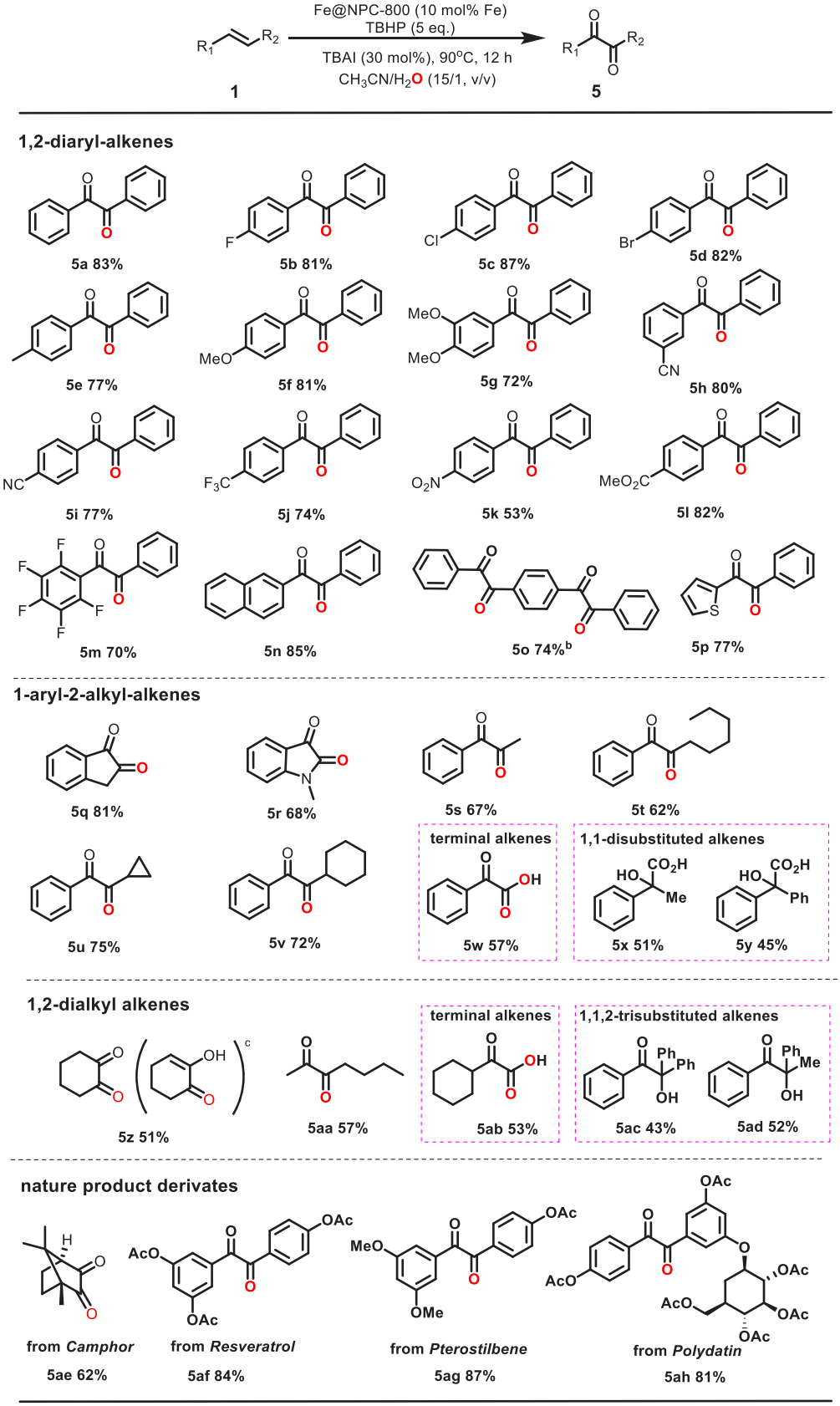

[a]Reaction conditions: alkene (0.2 mmol), Fe@NPC-800 (10 mol % of Fe), TBHP 70 wt % in water (5 equiv), TBAI (22.1 mg, 30 mol %), CH_3CN/H_2O (2 mL, v/v = 15/1), 90 °C, 12 h. [b]TBHP 70 wt % in water (10 equiv), 24 h. [c]Isomerization product was obtained. Yields of isolated product are reported.

https://dx.doi.org/10.1021/acscatal.9b05197
ACS Catal. 2020, 10, 4617−4629

Scheme 2. Applicability of One-Pot Cascade Reaction for Synthesis of Heterocycles Starting from Alkene

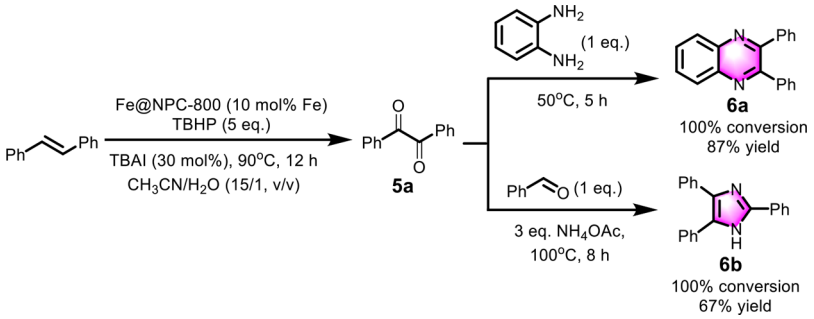

key building block for wide applications in synthesis of α-amino acids, pharmaceuticals, and agrochemicals,[20] which still remains a challenge in organic synthesis from readily available starting materials under facile and sustainable conditions. 1,1-Disubstituted alkenes (**1x'** and **1y'**) could be converted into the corresponding α-hydroxyl-acids (**5x** and **5y**) in 51% and 45% yields, respectively. Likewise, cycloalkenes and aliphatic alkenes, such as cyclohexene (**1z'**) and 2-octene (**1aa'**), are also suitable as substrates for the oxidation to 1,2-diketones. For the terminal aliphatic alkene, vinylcyclohexane (**1ab'**), was also oxidized into α-keto acid **5ab** in decent yield. Note that, 2-hydroxycyclohex-2-en-1-one (**5z**) was obtained via the isomerization of cyclohexane-1,2-dione. The α-hydroxyl-ketones (**5ac** and **5ad**) were obtained in moderate yields when using 1,1,2-trisunstituted alkenes (**1ac'** and **1ad'**) as substrates instead. In addition, several biologically active natural derivatives containing a C═C bond, e.g., Camphor (**1ae'**), Resveratrol (**1af'**), Pterostilbene (**1ag'**), and Polydatin (**1ah'**), can be efficiently oxidized into their respective 1,2-diketones in high yields. Overall, this method demonstrates a great substrate scope, highlighting its practical utility for direct synthesis of benzils from alkenes under mild and sustainable reaction conditions.

To further explore the applicability of this method, we carried out a one-pot cascade reaction starting from alkenes for the synthesis of biologically active heterocyclic compounds, such as 2,3-diphenylquinoxaline (**6a**) and 2,4,5-triphenyl-1H-imidazole (**6b**) (Scheme 2), because 1,2-diketones are well-known building blocks for such constructions.[21] After the full conversion of *trans*-stilbene under the optimized conditions, benzene-1,2-diamine or benzyl aldehyde/NH_4OAc was directly added into the reaction mixture for sequential condensation cyclization. To our delight, **6a** and **6b** were isolated in 87% and 67% yields, respectively. Comparatively, a considerably lower reactivity was achieved when the condensation was performed directly starting from benzil **5a** in the absence of the catalyst Fe@NPC-800 under otherwise identical conditions (Scheme S2). Such a finding is in line with previous reports[21c−f] and clearly indicates that the catalyst Fe@NPC-800 with Lewis acid sites could greatly facilitate the condensation, further highlighting its expanded potential.

3.3. Stability of the Catalyst Fe@NPC-800. The stability and reusability of the catalyst Fe@NPC-800 was also investigated. Upon completion of the benchmark oxidation reaction, the Fe@NPC-800 catalyst was easily separated from the product and recollected via centrifugation, and after washing and drying, it was used in subsequent cycles. As shown in Figure S13 in the Supporting Information, the catalyst exhibited good stability and could be easily separated and reused at least six times without significant loss of both the activity and selectivity, strongly indicating its robust stability.

3.4. Relationship between Catalytic Performance and Properties of the Catalyst. To better understand the reaction pathway of the oxidative cleavage of alkenes into a class of important ketones with one-carbon shorter, the benchmark reaction under the optimized conditions was further investigated. The product distribution as a function of reaction time (as shown in Figure 3) discloses that the

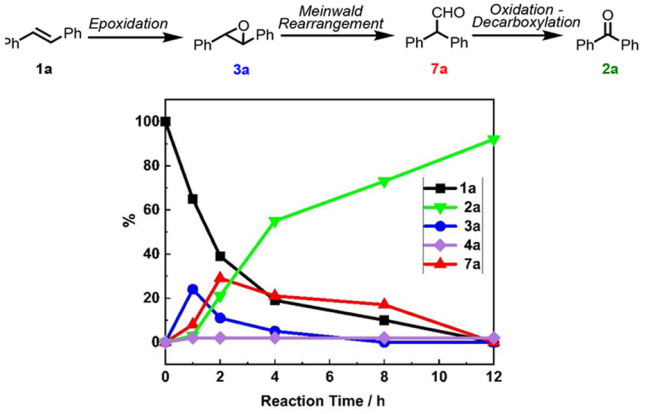

Figure 3. Product distribution of oxidation of *trans*-stilbene as a function of reaction times under the optimized conditions.

epoxidation of *trans*-stilbene **1a** with TBHP to produce epoxide **3a** dominates the reaction at the early stage in the presence of Fe@NPC-800 (within 1 h), accompanied by concomitant formation of diphenylacetaldehyde (**7a**) and benzophenone (**2a**). This may not be surprising because the Fe−N_x sites are key species in Fe@NPC-800, which structurally mimic Fe-porphyrin complexes and have been well-documented to efficiently enable alkene epoxidation.[22] With an elapse of reaction times, **1a** was consumed quickly and the formation of benzophenone **2a** prevailed, accompanied by the gradual conversion of both **3a** and **7a**. We subsequently correlated the content of Fe−N_x sites in the as-prepared catalysts Fe@NPC-*T* (*T* = 700, 800, and 900 °C) and the catalytic activities shown in Table S8 and found that the conversion of *trans*-stilbene **1a** highly depends on the content of Fe−N_x sites under otherwise identical conditions, indicating that Fe−N_x is indeed a catalytically active site for the oxidation of alkenes in the present catalytic system.

Interestingly, diphenylacetaldehyde **7a** as an intermediate was detected during the reaction course. This is reminiscent of the well-known Meinwald rearrangement of epoxide in the

https://dx.doi.org/10.1021/acscatal.9b05197
ACS Catal. 2020, 10, 4617−4629

presence of acid.[5] As such, a pyridine-adsorption FT-IR experiment for the catalyst Fe@NPC-800 was conducted. As shown in Figure 4, the spectrum discloses the presence of

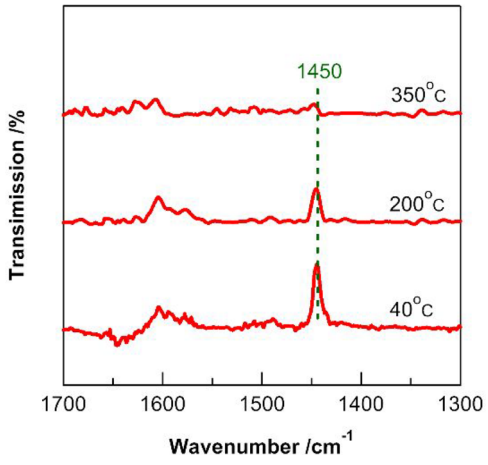

Figure 4. Pyridine-adsorption FT-IR spectra on the catalyst Fe@NPC-800 observed at varying temperatures.

Lewis acid sites on the catalyst, with the appearance of a characteristic peak at 1450 cm^{-1} and its concentration as high as 267.6 μmol per gram (Table S5), which most likely stem from the high valence of iron in $FePO_4$. The pyridine-poisoning experiment (Table S7) shows a considerable decrease of reactivity with 52% conversion of **1a**, with maintaining **3a** remaining as the major product due to the loss of the concentration of acid sites on the catalyst. An investigation on the catalytic activity and product selectivity (or distribution) over the catalysts Fe@NPC-700 and Fe@NPC-900 with different concentration of Lewis acid sites also gave similar results (Table 1, Table S8, and Figure S9), that is, a higher conversion of **1a** with a higher content of Fe−N_x sites, while better selectivity to **2a** with higher concentration of acid sites. This finding not only supports the presence of acid sites in the catalyst but also more importantly indicates that the acid sites exert a critical effect on reaction efficiency and product selectivity. For comparison, the catalyst Fe@NC-800 without the introduction of P was prepared according to the same preparation method, which gave a relatively lower reactivity and especially an inferior selectivity to **2a** under otherwise identical reaction conditions (Figure S9). The pyridine-adsorption FT-IR experiment also discloses that the Fe@NC-800 catalyst processes a relatively stronger concentration of Lewis acid sites (Figure S8 and Table S5). Such observations confirm that the addition of PPh_3 could facilitate the formation of $FePO_4$, giving rise to the Lewis acid sites. Further studies show that the reaction activity and selectivity to benzophenone follows a volcanic trend when varying the added amount of PPh_3 for catalyst preparation, with the 20 wt % loading giving the best catalytic activity (Figure S10).

3.5. Mechanistic Studies. Based on the results discussed above, we proposed a plausible reaction pathway, as shown in Scheme 3. First, an alkene is epoxidized by the Fe@NPC-800 catalyst with TBHP to generate an epoxide. Subsequently, the epoxide is converted to ketone with one-carbon shorter, in which sequential reactions take place, involving (i) a Lewis acid-catalyzed Meinwald rearrangement of the epoxide to an α-disubstituted acetaldehyde, (ii) oxidation of the aldehyde to a disubstituted acetic acid, (iii) decarboxylation of the acid with

Scheme 3. Proposed Mechanism for Oxidation of Alkenes to Ketones and 1,2-Diketones

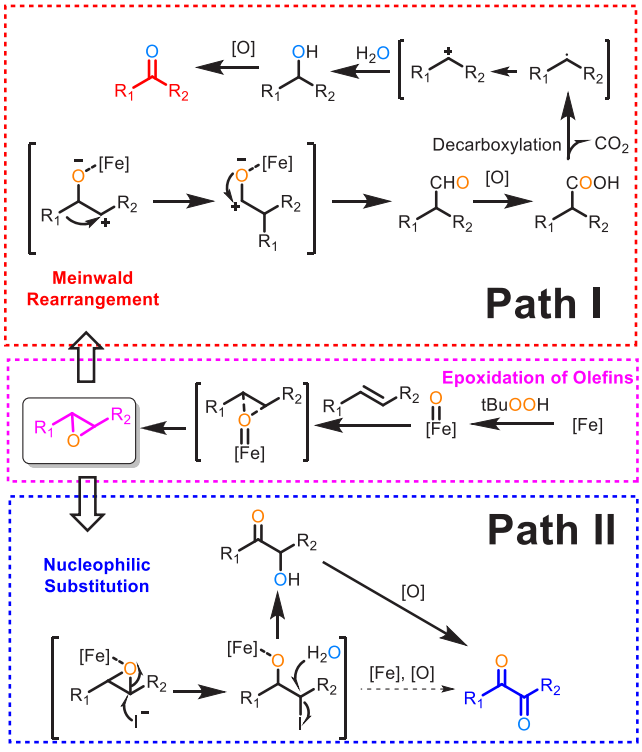

the loss of one carbon atom followed by one-electron oxidation of the resulting radical, and (iv) attachment at the carbon cation by water as nucleophile and further oxidation to produce a ketone.

To gain more evidence for this mechanism, a set of control experiments were subsequently carried out (Scheme 4).

Scheme 4. Control Experiments for the Synthesis of Ketones

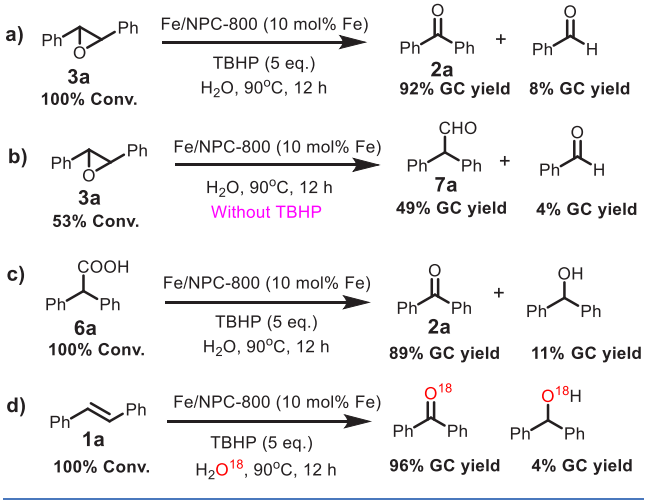

Stilbene epoxide **3a** could be efficiently converted toward benzophenone **2a** in 92% GC yield (84% isolated yield) under the optimized conditions (Scheme 4a), but in the absence of TBHP under otherwise identical conditions, only 53% conversion of **3a** was achieved, affording Meinwald rearranged product diphenylacetaldehyde **7a** in 49% GC yield (Scheme 4b). This observation indicates that TBHP as the oxidant

https://dx.doi.org/10.1021/acscatal.9b05197
ACS Catal. 2020, 10, 4617−4629

could accelerate selective conversion of epoxide to the desired ketones. Next, diphenylacetic acid **6a**, which is readily formed from oxidation of diphenylacetaldehyde **7a**, could also be effectively transferred into **2a** in 89% GC yield together with 11% of 1,2-diphenylmethanol and evolution of a CO_2 molecule (confirmed by GC analysis) (Scheme 4c). As is known, diphenylacetic acid can easily undergo oxidative decarboxylation into benzyl radical with the release of CO_2.[18] In the presence of an oxidant, the generated benzyl radical can be oxidized to carbocation, which can be easily attacked by a nucleophile like H_2O to form an alcohol and be further oxidized into ketone. To prove this, a $H_2{}^{18}O$ labeling experiment was performed (Scheme 4d and Figure S12). No appreciable difference in reactivity could be observed, and 96% of isolated yield of benzophenone was obtained with 100% ^{18}O labeling. Besides, 4% of diphenylmethanol with 100% ^{18}O labeling was also detected. This finding not only demonstrates that the origin of the oxygen atom in benzophenone and 1,2-diphenylmethanol stems from water rather than TBHP but also further proves that water indeed participates in the reaction as a nucleophile to attack the in situ generated decarboxylated intermediate (Scheme 3). Taking into account all these control experimental results, we may safely conclude that the proposed reaction pathway is most likely to be operative in our catalytic system (Scheme 3, Path I).

On the contrary, a competitive pathway of nucleophilic substitution prior to the Meinwald rearrangement is also possible if a strong nucleophile presents during the ring-opening of epoxide catalyzed by Lewis acid. If this is the case, the reaction would proceed following the pathway shown in Scheme 3, Path II. To investigate this possibility, new control experiments were conducted (Scheme 5). First, using 2-iodo-1,2-diphenylethan-1-one **A** as the substrate for the reaction under the optimized conditions (Scheme 5a), nearly quantitative yield to benzil **5a** was observed. The iodide in **A**, as a good leaving group, can be readily substituted by water to produce 2-hydroxy-1,2-diphenylethan-1-one **B** in a CH_3CN/H_2O mixture at 90 °C (Scheme 5b), which can be quantitatively converted into **5a** under the optimized conditions (Scheme 5c). In contrast, a considerably lower reactivity was observed when **A** was subjected to the optimized conditions in the absence of water (Scheme 5d), indicating that H_2O as a nucleophile is favorable for the reaction process. Taking all the results together, we considered that the proposed reaction pathway illustrated in Scheme 3, Path II was feasible.

Scheme 5. Control Experiments for the Synthesis of 1,2-Diketones

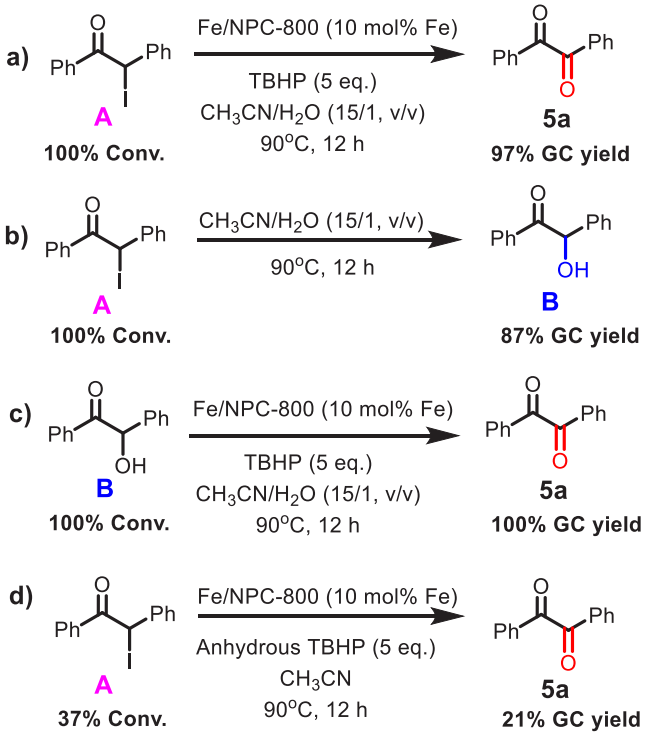

4. CONCLUSIONS

In conclusion, we have developed a novel, inexpensive bifunctional iron nanocomposite catalyst in a facile and environmentally friendly manner. Two key iron species, Fe–N_x and $FePO_4$ as the oxidation and acid sites, respectively, were simultaneously integrated on the hierarchical porous carbon, which are primarily responsible for the direct oxidative cleavage of alkenes via the formation of epoxide as the key intermediate. A broad range of alkenes could be efficiently converted into industrially important ketones and 1,2-diketones with good tolerance of functional groups using TBHP as the oxidant under mild reaction conditions. In addition, the catalyst can be readily recovered for successive recycles. This study provides a simple and efficient method for the synthesis of synthetically significant ketones and 1,2-diketones from the direct oxidation of alkenes in a cost-effective and environmentally friendly manner, and we believe the method would be very useful in the synthesis of fine chemicals, pharmaceuticals, agrochemicals, and materials.

■ ASSOCIATED CONTENT

Supporting Information

The Supporting Information is available free of charge at The Supporting Information is available free of charge at https://pubs.acs.org/doi/10.1021/acscatal.9b05197.

Discussions of materials and methods used, preparations, isotopic labelling experiments, recyclability, equations, and characterization of products, figures of XRD patterns, Raman spectra, magnetic hysteresis curves, N_2 sorption isotherms, pore size distribution, high-resolution XPS spectra, Fe nanoarticle size distribution, FT-IR spectra, conversion and product selectivity, catalytic performance, GC–MS spectra, recyclability of the catalyst, product distribution, and ^1H and ^{13}C NMR spectra, table of average pore size, chemical composition and textural properties, nitrogen types and respective contents in carbon matrix, P types and respective contents in carbon matrix, concentrations of Lewis acid sites, optimization of reaction conditions, pyridine-poisoning experiment results, correlation of catalytic performance and selectivity, carbon balance for synthesis of ketones, and catalytic activity, and schemes of one-pot cascade reactions, synthesis of heterocycles, and control experiments of Meinwald rearrangement (PDF)

https://dx.doi.org/10.1021/acscatal.9b05197
ACS Catal. 2020, 10, 4617–4629

AUTHOR INFORMATION

Corresponding Authors

Jianliang Xiao − *Department of Chemistry, University of Liverpool, Liverpool L69 7ZD, United Kingdom;* orcid.org/0000-0003-2010-247X; Email: j.xiao@liverpool.ac.uk

Yong Yang − *CAS Key Laboratory of Bio-Based Materials, Qingdao Institute of Bioenergy and Bioprocess Technology, Chinese Academy of Sciences, Qingdao 266101, China;* orcid.org/0000-0002-6118-5200; Email: yangyong@qibebt.ac.cn

Authors

Tao Song − *CAS Key Laboratory of Bio-Based Materials, Qingdao Institute of Bioenergy and Bioprocess Technology, Chinese Academy of Sciences, Qingdao 266101, China;* orcid.org/0000-0003-2088-8177

Zhiming Ma − *CAS Key Laboratory of Bio-Based Materials, Qingdao Institute of Bioenergy and Bioprocess Technology, Chinese Academy of Sciences, Qingdao 266101, China; University of Chinese Academy of Sciences, Beijing 100049, China*

Peng Ren − *CAS Key Laboratory of Bio-Based Materials, Qingdao Institute of Bioenergy and Bioprocess Technology, Chinese Academy of Sciences, Qingdao 266101, China; University of Chinese Academy of Sciences, Beijing 100049, China;* orcid.org/0000-0002-5767-2938

Youzhu Yuan − *State Key Laboratory of Physical Chemistry of Solid Surfaces, National Engineering Laboratory for Green Chemical Production of Alcohols-Ethers-Esters, College of Chemistry and Chemical Engineering, Xiamen 361005, P. R. China;* orcid.org/0000-0003-1668-9984

Complete contact information is available at: https://pubs.acs.org/10.1021/acscatal.9b05197

Notes

The authors declare no competing financial interest.

ACKNOWLEDGMENTS

The authors would like to acknowledge the financial support from the Key Technology R&D Program of Shandong Province (2019GGX102075), DICP & QIBEBT (Grant No. DICP & QIBEBT UN201704), and the Dalian National Laboratory for Clean Energy (DNL) Cooperation Fund, CAS (Grant No. DNL201904), Open Projects of State Key Laboratory of Physical Chemistry of the Solid State Surface (Xiamen University) (No. 201808). Y.Y also acknowledges the Royal Society (UK) for a Newton Advanced Fellowship (NAF \R2\180695)

REFERENCES

(1) (a) Cuquerella, M. C.; Lhiaubet-Vallet, V.; Cadet, J.; Miranda, M. A. Benzophenone Photosensitized DNA Damage. *Acc. Chem. Res.* **2012**, *45*, 1558. (b) Kamat, P. V. Photochemistry on Nonreactive and Reactive (Semiconductor) Surfaces. *Chem. Rev.* **1993**, *93*, 267. (c) Maurya, R.; Singh, R.; Deepak, M.; Handa, S. S.; Yadav, P. P.; Mishra, P. K. Constituents of Pterocarpus Marsupium: an Ayurvedic Crude Drug. *Phytochemistry* **2004**, *65*, 915. (d) Deng, X.; Mani, N. An Efficient Route to 4-Aryl-5-pyrimidinylimidazoles via Sequential Functionalization of 2, 4-Dichloropyrimidine. *Org. Lett.* **2006**, *8*, 269. (e) Wolkenberg, S. E.; Wisnoski, D. D.; Leister, W. H.; Wang, Y.; Zhao, Z.; Lindsley, C. W. Efficient Synthesis of Imidazoles from Aldehydes and 1, 2-Diketones using Microwave Irradiation. *Org. Lett.* **2004**, *6*, 1453. (f) Slee, D. H.; Romano, S. J.; Yu, J.; Nguyen, T. N.; John, J. K.; Raheja, N. K.; Axe, F. U.; Jones, T. K.; Ripka, W. C. Development of Potent Non-Carbohydrate Imidazole-Based Small Molecule Selectin Inhibitors with Anti-inflammatory Activity. *J. Med. Chem.* **2001**, *44*, 2094. (g) Wright, M. W.; Welker, M. E. Transition Metal Mediated *exo* Selective Diels-alder Reactions: Preparation of 2-Cobalt-Substituted 1,3-Dienes Containing C_2 Symmetric 2,3-Dibenzobicyclo[2.2.2]octanedione Dioxime Equatorial Ligands and Their Use in Thermal and Lewis Acid Catalyzed 4 + 2 Cycloadditions. *J. Org. Chem.* **1996**, *61*, 133. (h) Li, X.; Jiao, N. The Reoxidation of Transition-Metal Catalysts with O_2. *Chin. J. Chem.* **2017**, *35*, 1349. (i) Liang, W.; Zhang, Z.; Yi, D.; Fu, Q.; Chen, S.; Yang, L.; Du, F.; Ji, J.; Wei, W. Copper-Catalyzed Direct Oxyphosphorylation of Enamides with P(O)-H Compounds and Dioxygen. *Chin. J. Chem.* **2017**, *35*, 1378.

(2) Selected examples for synthesis of ketones from oxidation of alkenes: (a) Knops-Gerrits, P.-P.; Vos, D. D.; Thibault-Starzyk, F.; Jacobs, P. A. Zeolite-encapsulated Mn (II) Complexes as Catalysts for Selective Alkene Oxidation. *Nature* **1994**, *369*, 543. (b) Fraile, J. M.; García, N.; Mayoral, J. A.; Santomauro, F. G.; Guidotti, M. Multifunctional Catalysis Promoted by Solvent Effects: Ti-MCM41 for a One-Pot, Four-Step, Epoxidation-Rearrangement-Oxidation-Decarboxylatio Reaction Sequence on Stilbenes and Styrenes. *ACS Catal.* **2015**, *5*, 3552. (c) Zeng, X.; Xu, D.; Miao, C.; Xia, C.; Sun, W. Tetraethylammonium Iodide Catalyzed Synthesis of Diaryl Ketones via the Merger of Cleavage of C-C Double Bonds and Recombination of Aromatic Groups. *RSC Adv.* **2014**, *4*, 46494. (d) Sharma, N.; Sharma, A.; Kumar, R.; Shard, A.; Sinha, A. K. One-Pot Two-Step Oxidative Cleavage of 1,2-Arylalkenes to Aryl ketones Instead of Arylaldehydes in an Aqueous Medium: a Complementary Approach to Ozonolysis. *Eur. J. Org. Chem.* **2010**, *2010*, 6025.

(3) Selected examples for synthesis of 1,2-diketones from oxidation of alkenes: (a) Ren, W.; Liu, J.; Chen, L.; Wan, X. Ruthenium-Catalyzed Alkyne Oxidation with Part-Per-Million Catalyst Loadings. *Adv. Synth. Catal.* **2010**, *352*, 1424. (b) Chen, S.; Liu, Z.; Shi, E.; Chen, L.; Wei, W.; Li, H.; Cheng, Y.; Wan, X. Ruthenium-Catalyzed Oxidation of Alkenes at Room Temperature: a Practical and Concise Approach to α-Diketones. *Org. Lett.* **2011**, *13*, 2274. (c) Liu, X.; Chen, W. Pyridazine-Based *N*-Heterocyclic Carbene Complexes and Ruthenium-Catalyzed Oxidation Reaction of Alkenes. *Organometallics* **2012**, *31*, 6614. (d) Basavaraju, K. C.; Sharma, S.; Singh, A. K.; Im, D. J.; Kim, D.-P. Chitosan-Microreactor: a Versatile Approach for Heterogeneous Organic Synthesis in Microfluidics. *ChemSusChem* **2014**, *7*, 1864. (e) Mori, S.; Takubo, M.; Yanase, T.; Maegawa, T.; Monguchi, Y.; Sajikia, H. Palladium on Carbon-Catalyzed Synthesis of Benzil Derivatives from 1,2-Diarylalkynes with DMSO and Molecular Oxygen as Dual Oxidants. *Adv. Synth. Catal.* **2010**, *352*, 1630. (f) Firouzabadi, H.; Sardarian, A. R.; Moosavipour, H.; Afshari, G. M. Chromium (VI) Based Oxidants; II. Zinc Dichromate Trihydrate: a Versatile and Mild Reagent for the Oxidation of Organic Compounds. *Synthesis* **1986**, *1986*, 285. (g) Tamuli, K. J.; Bordoloi, M. KI-I_2-DMSO: an Improved Microwave-Assisted Selective Oxidation of Alkenes into 1,2-Diketones. *ChemistrySelect* **2018**, *3*, 7513. (h) Moorthy, J. N.; Nidhi, S.; Kalyan, S. Oxidations with IBX: Benzyl Halides to Carbonyl Compounds, and the One-Pot Conversion of Olefins to 1, 2-Diketones. *Tetrahedron Lett.* **2006**, *47*, 1757. (i) Clayton, M. D.; Marcinow, Z.; Rabideau, P. W. Benzeneselenic Anhydride Oxidation of 1,2-Diarylethanes and 1,2-Diarylethylenes to 1,2-Diaryldiketones. *Tetrahedron Lett.* **1998**, *39*, 9127. (j) Su, Y.; Sun, X.; Wu, G.; Jiao, N. Catalyst-Controlled Highly Selective Coupling and Oxygenation of Olefins: a Direct Approach to Alcohols, Ketones, and Diketones. *Angew. Chem., Int. Ed.* **2013**, *52*, 9808. (k) Andia, A. A.; Miner, M. R.; Woerpel, K. A. Copper(I)-Catalyzed Oxidation of Alkenes Using Molecular Oxygen and Hydroxylamines: Synthesis and Reactivity of α-Oxygenated ketones. *Org. Lett.* **2015**, *17*, 2704. (l) Saberi, D.; Hashemi, H.; Niknam, K. One-Pot Solvent-Free Synthesis of Diaryl 1,2-Diketones by the Sequential Heck Oxidation Reaction of Aryl Halides with Styrenes. *Asian J. Org. Chem.* **2017**, *6*, 169.

(4) (a) Lee, M.; Lamb, J. R.; Sanford, M. J.; LaPointe, A. M.; Coates, G. W. Nucleophilic Ring Opening of Trans-2,3-disubstituted

Epoxides to β-Amino Alcohols with Catalyst-Controlled Regioselectivity. *Chem. Commun.* **2018**, *54*, 12998. (b) Gava, R.; Fernndez, E. Selective C-C Coupling of Vinyl Epoxides with Diborylmethide Lithium Salts. *Chem. - Eur. J.* **2019**, *25*, 1. (c) Jacobsen, E. N. Asymmetric Catalysis of Epoxide Ring-Opening Reactions. *Acc. Chem. Res.* **2000**, *33*, 421.

(5) (a) Tiddens, M. R.; Gebbink, R. J. M. K.; Otte, M. The $B(C_6F_5)_3$-Catalyzed Tandem Meinwald Rearrangement-Reductive Amination. *Org. Lett.* **2016**, *18*, 3714. (b) Shen, Y.-M.; Wang, B.; Shi, Y. Enantioselective Synthesis of 2-Aryl Cyclopentanones by Asymmetric Epoxidation and Epoxide Rearrangement. *Angew. Chem., Int. Ed.* **2006**, *45*, 1429. (c) Zhu, B.; Shen, T.; Huang, X.; Zhu, Y.; Song, S.; Jiao, N. Highly Selective Aerobic Oxygenation of Tertiary Allylic Alcohols with Molecular Oxygen. *Angew. Chem., Int. Ed.* **2019**, *58*, 11028.

(6) (a) Magnus, A.; Bertilsson, S. K.; Andersson, P. G. Asymmetric Base-Mediated Epoxide Isomerization. *Chem. Soc. Rev.* **2002**, *31*, 223. (b) Lumbroso, A.; Cooke, M. L.; Breit, B. Catalytic Asymmetric Synthesis of Allylic Alcohols and Derivatives and Their Applications in Organic Synthesis. *Angew. Chem., Int. Ed.* **2013**, *52*, 1890.

(7) (a) Banerjee, D.; Jagadeesh, R. V.; Junge, K.; Pohl, M. M.; Radnik, J. Convenient and Mild Epoxidation of Alkenes Using Heterogeneous Cobalt Oxide Catalysts. *Angew. Chem., Int. Ed.* **2014**, *53*, 4359. (b) Lane, B. S.; Burgess, K. Metal-Catalyzed Epoxidations of Alkenes with Hydrogen Peroxide. *Chem. Rev.* **2003**, *103*, 2457. (c) White, M. C.; Doyle, A. G.; Jacobsen, E. N. A Synthetically Useful, Self-Assembling MMO Mimic System for Catalytic Alkene Epoxidation with Aqueous H_2O_2. *J. Am. Chem. Soc.* **2001**, *123*, 7194. (d) Miao, C.; Wang, B.; Wang, Y.; Xia, C.; Lee, Y.-M.; Nam, W.; Sun, W. Proton-Promoted and Anion-Enhanced Epoxidation of Olefins by Hydrogen Peroxide in the Presence of Nonheme Manganese Catalysts. *J. Am. Chem. Soc.* **2016**, *138*, 936. (e) Tada, M.; Muratsugu, S.; Kinoshita, S.; Sasaki, T.; Iwasawa, Y. Alternative Selective Oxidation Pathways for Aldehyde Oxidation and Alkene Epoxidation on a SiO_2-Supported Ru-Monomer Complex Catalyst. *J. Am. Chem. Soc.* **2010**, *132*, 713. (f) Cui, T.-L.; Li, X.-H.; Chen, J.-S. Mesoporous TS-1 Nanocrystals as Low Cost and High Performance Catalysts for Epoxidation of Styrene. *Chin. J. Chem.* **2017**, *35*, 577.

(8) (a) Duan, Y.; Dong, X.; Song, T.; Wang, Z.; Xiao, J.; Yuan, Y.; Yang, Y. Hydrogenation of Functionalized Nitroarenes Catalyzed by Single-Phase Pyrite FeS_2 Nanoparticles on N, S-Codoped Porous Carbon. *ChemSusChem* **2019**, *12*, 4636. (b) Ma, Z.; Song, T.; Yuan, Y.; Yang, Y. Synergistic Catalysis on Fe-N_x Sites and Fe Nanoparticles for Efficient Synthesis of Quinolines and Quinazolinones via Oxidative Coupling of Amines and Aldehydes. *Chem. Sci.* **2019**, *10*, 10283. (c) Song, T.; Ren, P.; Duan, Y.; Wang, Z.; Chen, X.; Yang, Y. Cobalt Nanocomposites on N-Doped Hierarchical Porous Carbon for Highly Selective Formation of Anilines and Imines from Nitroarenes. *Green Chem.* **2018**, *20*, 4629. (d) Duan, Y.; Song, T.; Dong, X.; Yang, Y. Enhanced Catalytic Performance of Cobalt Nanoparticles Coated with a N, P-Codoped Carbon Shell Derived from Biomass for Transfer Hydrogenation of Functionalized Nitroarenes. *Green Chem.* **2018**, *20*, 2821.

(9) (a) Mun, Y.; Lee, S.; Kim, K.; Kim, S.; Lee, S.; Han, J. W.; Lee, J. Versatile Strategy for Tuning ORR Activity of a Single Fe-N Site by Controlling Electron Withdrawing/Donating Properties of Carbon Plane. *J. Am. Chem. Soc.* **2019**, *141*, 6254. (b) Jiang, W.-J.; Gu, L.; Li, L.; Zhang, Y.; Zhang, X.; Zhang, L.-J.; Wang, J.-Q.; Hu, J.-S.; Wei, Z.; Wan, L.-J. Understanding the High Activity of Fe-N-C Electrocatalysts in Oxygen Reduction: Fe/Fe_3C Nanoparticles Boost the Activity of Fe-N_x. *J. Am. Chem. Soc.* **2016**, *138*, 3570.

(10) Yan, Y.; Zhao, B.; Yi, S. C.; Wang, X. Assembling Pore-Rich FeP Nanorods on the CNT Backbone as an Advanced Electrocatalyst for Oxygen Evolution. *J. Mater. Chem. A* **2016**, *4*, 13005.

(11) (a) Yang, D.-S.; Bhattacharjya, D.; Inamdar, S.; Park, J.; Yu, J.-S. Phosphorus-Doped Ordered Mesoporous Carbons with Different Lengths as Efficient Metal-Free Electrocatalysts for Oxygen Reduction in Alkaline Media. *J. Am. Chem. Soc.* **2012**, *134*, 16127. (b) Zhang, J.; Zhao, Z.; Xia, Z.; Dai, L. A Metal-Free Bifunctional Electrocatalyst for Oxygen Reduction and Oxygen Evolution Reactions. *Nat. Nanotechnol.* **2015**, *10*, 444. (c) Barbaux, Y.; Dekiouk, M. Bulk and Surface Analysis of a Fe-P-O Oxydehydrogenation Catalyst. *Appl. Catal., A* **1992**, *90*, 51.

(12) (a) Du, X.; He, W.; Zhang, X.; Yue, Y.; Liu, H.; Zhang, X.; Min, D.; Ge, X.; Du, Y. Enhancing the Electrochemical Performance of Lithium Ion Batteries Using Mesoporous $Li_3V_2(PO_4)_3$/C Microspheres. *J. Mater. Chem.* **2012**, *22*, 5960. (b) Ravikumar, B.; Ramaswamy, S.; Jinnah, M. A.; Rajaram, R. K.; Ramakrishnan, V. Raman and Infrared Spectral Studies of DL-Threoninium Dihydrogenphosphate. *J. Raman Spectrosc.* **2004**, *35*, 847.

(13) Serov, A.; Artyushkova, K.; Atanassov, P. Fe-N-C Oxygen Reduction Fuel Cell Catalyst Derived from Carbendazim: Synthesis, Structure, and Reactivity. *Adv. Energy Mater.* **2014**, *4*, 1301735.

(14) Asakura, D.; Nanba, Y.; Makinose, Y.; Matsuda, H.; Glans, P.; Guo, J.; Hosono, E. Large Charge-Transfer Energy in $LiFePO_4$ Revealed by Full-Multiplet Calculation for the Fe L_3-edge Soft X-Ray Emission Spectra. *ChemPhysChem* **2018**, *19*, 988.

(15) (a) Wu, G.; More, K. L.; Johnston, C. M.; Zelenay, P. High-Performance Electrocatalysts for Oxygen Reduction Derived from Polyaniline, Iron, and Cobalt. *Science* **2011**, *332*, 443. (b) Yang, J.; Liu, D.-J.; Kariuki, N. N.; Chen, L. X. Aligned Carbon Nanotubes with Built-in FeN_4 Active Sites for Electrocatalytic Reduction of Oxygen. *Chem. Commun.* **2008**, 329.

(16) Wang, F.; Cao, X.; Mei, L.; Zhang, X.; Hu, J.; Yan, T. Twisted Penta-carbazole/Benzophenone Hybrid Compound as Multifunctional Organic Host, Dopant or Non-Doped Emitter for Highly Efficient Solution Processed Delayed Fluorescence OLEDs. *Chin. J. Chem.* **2018**, *36*, 241.

(17) Tang, H.; Huang, B.; Xie, X.; Yan, T.; Cai, M. Synthesis and Properties of Novel Soluble Fluorinated Aromatic Polyamides Containing 4-Benzoyl-2, 3, 5, 6-Tetrafluorophenoxy Pendant Groups. *J. Polym. Res.* **2018**, *25*, 51.

(18) (a) Wang, Z.; Zhu, L.; Yin, F.; Su, Z.; Li, Z.; Li, C. Silver-Catalyzed Decarboxylative Chlorination of Aliphatic Carboxylic Acids. *J. Am. Chem. Soc.* **2012**, *134*, 4258. (b) Song, Q.; Feng, Q.; Yang, K. Synthesis of Primary Amides via Copper-Catalyzed Aerobic Decarboxylative Ammoxidation of Phenylacetic Aids and α-Hydroxyphenylacetic Acids with Ammonia in Water. *Org. Lett.* **2014**, *16*, 624.

(19) (a) Chang, J.; Shin, E.; Kim, H. j.; Kim, Y.; Park, Y. S. Stereoselective Syntheses of Tri- and Tetrapeptide Analogues by Dynamic Resolution of α-Halo Amides in Nucleophilic Substitution. *Tetrahedron* **2005**, *61*, 2743. (b) von Angerer, S.; von Angerer, E.; Ambros, R.; Wiegrebe, W. Ring-Cleavage of Phthalidisoquinoline Alkaloids by Ethyl Chloroformate. *Arch. Pharm.* **1992**, *325*, 425.

(20) (a) Iding, H.; Siegert, P.; Mesch, K.; Pohl, M. Application of α-Keto Acid Decarboxylases in Biotransformations. *Biochim. Biophys. Acta, Protein Struct. Mol. Enzymol.* **1998**, *1385*, 307. (b) Krix, G.; Bommarius, A. S.; Drauz, K.; Kottenhahn, M.; Schwarm, M.; Kula, M.-R. Enzymatic Reduction of α-Keto Acids Leading to l-Amino Acids, d- or l-Hydroxy acids. *J. Biotechnol.* **1997**, *53*, 29. (c) Angata, T.; Varki, A. Chemical Diversity in the Sialic Acids and Related α-Keto Acids: an Evolutionary Perspective. *Chem. Rev.* **2002**, *102*, 439. (d) Penteado, F.; Lopes, E. F.; Alves, D.; Perin, G.; Jacob, R. G.; Lenardã, E. J. α-Keto Acids: Acylating Agents in Organic Synthesis. *Chem. Rev.* **2019**, *119*, 7113.

(21) (a) Schmidt, B.; Krehl, S.; Hauke, S. Assisted Tandem Catalytic Cross Metathesis-Oxidation: in One Flask from Styrenes to 1, 2-Diketones and Further to Quinoxalines. *J. Org. Chem.* **2013**, *78*, 5427. (b) Wolkenberg, S. E.; Wisnoski, D. D.; Leister, W. H.; Wang, Y.; Zhao, Z.; Lindsley, C. W. Efficient Synthesis of Imidazoles from Aldehydes and 1, 2-Diketones using Microwave Irradiation. *Org. Lett.* **2004**, *6*, 1453. (c) Aghapoor, K.; Mohsenzadeh, F.; Shakeri, A.; Darabi, H. R.; Ghassemzadeh, M.; Neumüller, B. Catalytic Application of Recyclable Silica-Supported Bismuth (III) Chloride in the Benzo [N, N]-Heterocyclic Condensation. *J. Organomet. Chem.* **2013**, *743*, 170. (d) Hamidi, Z.; Zarchi, M. A. K. Synthesis of Polymer-Supported Fe_3O_4 Nanoparticles and Their Application as a Novel Route for the Synthesis of Imidazole Derivatives. *Res. Chem.*

https://dx.doi.org/10.1021/acscatal.9b05197
ACS Catal. 2020, 10, 4617−4629

Intermed. **2018**, *44*, 6995. (e) Kumari, M.; Jain, Y.; Yadav, P.; Laddha, H.; Gupta, R. Synthesis of Fe_3O_4-DOPA-Cu Magnetically Separable Nanocatalyst: a Versatile and Robust Catalyst for an Array of Sustainable Multicomponent Reactions Under Microwave Irradiation. *Catal. Lett.* **2019**, *149*, 2180. (f) Zarnegar, Z.; Safari, J. Catalytic Activity of Cu Nanoparticles Supported on Fe_3O_4-Polyethylene Glycol Nanocomposites for the Synthesis of Substituted Imidazoles. *New J. Chem.* **2014**, *38*, 4555. (g) Nejatianfar, M.; Akhlaghinia, B.; Jahanshahi, R. Cu(II) Immobilized on Guanidinated Epibromohydrin-Functionalized γ-Fe_2O_3@TiO (γ-Fe_2O_3@TiO_2-EG-Cu(II)): a Highly Efficient Magnetically Separable Heterogeneous Nanocatalyst for One-Pot Synthesis of Highly Substituted Imidazoles. *Appl. Organomet. Chem.* **2018**, *32*, e4095.

(22) (a) Adam, W.; Stegmann, V. R.; Saha-Moller, C. R. Regio- and Diastereoselective Epoxidation of Chiral Allylic Alcohols Catalyzed by Manganese(salen) and Iron(porphyrin) Complexes. *J. Am. Chem. Soc.* **1999**, *121*, 1879. (b) Collman, J. P.; Wang, Z.; Straumanis, A.; Quelquejeu, M.; Rose, E. An Efficient Catalyst for Asymmetric Epoxidation of Terminal Olefins. *J. Am. Chem. Soc.* **1999**, *121*, 460. (c) Machii, K.; Watanabe, Y.; Morishima, I. Acylperoxo-Iron (III) Porphyrin Complexes: a New Entry of Potent Oxidants for the Alkene Epoxidation. *J. Am. Chem. Soc.* **1995**, *117*, 6691.

https://dx.doi.org/10.1021/acscatal.9b05197
ACS Catal. 2020, 10, 4617−4629